European Radiology (2019) 29:5341–5348
https://doi.org/10.1007/s00330-019-06130-x

CHEST

# Application of deep learning–based computer-aided detection system: detecting pneumothorax on chest radiograph after biopsy

Sohee Park[1] · Sang Min Lee[1] · Namkug Kim[2] · Jooae Choe[1] · Yongwon Cho[2] · Kyung-Hyun Do[1] · Joon Beom Seo[1]

Received: 28 September 2018 / Revised: 9 January 2019 / Accepted: 6 March 2019 / Published online: 26 March 2019


## Abstract

**Objectives** To retrospectively evaluate the diagnostic performance of a convolutional neural network (CNN) model in detecting pneumothorax on chest radiographs obtained after percutaneous transthoracic needle biopsy (PTNB) for pulmonary lesions.

**Methods** A CNN system for computer-aided diagnosis on chest radiographs was developed using the full 26-layer You Only Look Once model. A total of 1596 chest radiographs with pneumothorax were used for training. To validate the clinical feasibility of this model, follow-up chest radiographs obtained after PTNB for 1333 pulmonary lesions in 1319 patients in 2016 were prepared as an independent test set. Two experienced radiologists determined the presence of pneumothorax by consensus. The diagnostic performance of the CNN model was assessed using the jackknife free-response receiver operating characteristic method.

**Results** The incidence of pneumothorax was 17.9% (247/1379) on 3-h follow-up chest radiographs and 23.3% (309/1329) on 1-day follow-up chest radiographs. Twenty-three (1.7% of all PTNBs) cases required drainage catheter insertion. Our approach had a sensitivity, a specificity, and an area under the curve (AUC), respectively, of 61.1% (151/247), 93.0% (1053/1132), and 0.898 for 3-h follow-up chest radiographs and 63.4% (196/309), 93.5% (954/1020), and 0.905 for 1-day follow-up chest radiographs. The overall accuracy was 87.3% (1204/1379) for 3-h follow-up radiographs and 86.5% (1150/1329) for 1-day follow-up radiographs. The CNN model found all 23 cases of pneumothorax requiring drainage.

**Conclusions** Our CNN model had good performance for detection of pneumothorax on chest radiographs after PTNB, especially for those requiring further procedures. It can be used as a screening tool prior to radiologist interpretation.

**Key Points**

- *The CNN model had good performance for detection of pneumothorax on chest radiographs after PTNB and showed high specificity and negative predictive value.*
- *The CNN model found all cases of pneumothorax requiring drainage after PTNB.*
- *The CNN model can be used as a screening tool prior to radiologist interpretation.*

**Keywords** Machine learning · Radiography · Lung · Biopsy · Pneumothorax

Sang Min Lee and Namkug Kim contributed equally to this work.

✉ Sang Min Lee
sangmin.lee.md@gmail.com

✉ Namkug Kim
namkugkim@gmail.com

[1] Department of Radiology and Research Institute of Radiology, Asan Medical Center, College of Medicine, University of Ulsan, 88 Olympic-ro 43 Gil, Songpa-gu, Seoul 138736, South Korea

[2] Department of Convergence Medicine, Asan Medical Center, College of Medicine, University of Ulsan, 88, Olympic-ro 43-gil, Seoul 05505, South Korea

**Abbreviations**

| | |
|---|---|
| AUC | Area under the curve |
| CNN | Convolutional neural network |
| JAFROC | Jackknife free-response receiver operating characteristic |
| PTNB | Percutaneous transthoracic needle biopsy |

## Introduction

Percutaneous transthoracic needle biopsy (PTNB) is a well-established and commonly used method for the diagnosis of pulmonary lesions and has a high diagnostic accuracy of

92.0% to 97.0% [1–3]. In performing PTNB, the most common complication is pneumothorax. The incidence of pneumothorax has ranged from 17.0% to 38.3% [1, 3, 4]. Although chest tube drainage is required in a small number of PTNBs (1.1–1.4%) [3, 4], early detection of pneumothorax and prompt treatment are clinically important for patient care. However, high case loads in radiology practices make it difficult to have timely attention and early recognition of critical imaging findings. Automated detection algorithms have attracted attention in efforts to address these unmet clinical needs.

Regarding this, Geva et al [5] have reported that a texture analysis–based method achieved 81% sensitivity and 87% specificity for the detection of pneumothorax on a dataset of 108 chest radiographs. Chan et al [6] also reported that an automatic detection method using image multiscale intensity analysis and segmentation had an accuracy of 76.9–88.4% for 26 cases after training using 58 cases.

Recently, Cicero et al [7] applied convolutional neural network (CNN), which is one of the deep learning algorithms, to chest radiographs. This method had a sensitivity of 78%, a specificity of 78%, and an area under the curve (AUC) of 0.861 for the detection of pneumothorax in 167 cases after training using 1299 pneumothorax images [7]. Blumenfeld et al [8] achieved high diagnostic accuracy with an AUC of 0.95 using a CNN model based on pixel classification, even when given a relatively small training dataset (117 chest radiographs).

However, these studies used relatively small numbers of cases for validation and did not carefully consider clinical scenarios such as clear and consistent inclusion criteria, prevalence of events, or target population for validation. Therefore, the clinical performance of CNN for detection of pneumothorax should be assessed in a large target population with use cases before clinical application. The purpose of this study was to retrospectively assess the diagnostic performance of a CNN model for detection of pneumothorax on chest radiographs after PTNB for pulmonary lesions.

## Materials and methods

This retrospective study was approved by the institutional review board, which waived the requirement for informed consent (IRB number: 2018-0708).

### Datasets for the deep learning–based model

A total of 1596 chest radiographs of cases of pneumothorax at different levels of severity and 11,137 chest radiographs of normal cases from two tertiary referral hospitals were collected from a picture archiving and communication system to develop the CNN model. Diagnoses were searched using the radiologic reports and diagnosis codes in the electronic medical records. All normal chest radiographs were confirmed through chest CT performed on the same day. A total of 1343 images of pneumothorax were randomly split at 9:1 ratio into training and validation datasets. Additional 253 images of pneumothorax and 250 normal chest radiographs were used for internal validation. After anonymization of images, two thoracic radiologists (J.C. and S.M.L. with 6 years and 10 years of experience in thoracic radiology, respectively) manually drew regions of interest for cases of pneumothorax using in-house software.

### Development of deep learning–based model

Before training of CNN, we needed to carefully redesign workflows on preprocessing, deep neural network architecture, and computing hardware setting. Histograms of X-ray images were extracted and used for preprocessing with contrast-limited adaptive histogram equalization using a 0.1% rescale of the scikit-image in Python 2.7. Chest X-ray images and region of interest masks were resized from 2000 × 2000 matrices to 1000 × 1000 matrices and converted to 16-bit portable network graphics format.

The CNN was trained using a chest X-ray image with strong label, which was manually generated by two thoracic radiologists. The network used for the inferences was fine-tuned using the You Only Look Once (YOLO Darknet19) pretrained model (Fig. 1) [9]. We used the randomly selected 10% of the 1343 images of the training and validation datasets to determine the model with the lowest validation loss and optimized the final weights with a stochastic gradient descent (SGD) method. Lastly, we predicted the location and classification of pneumothorax in all test datasets. In YOLO, each image is divided into an $S \times S$ grid and directly regressed to determine bounding boxes for the lesions, the confidence for the boxes, and a score for each probability within each grid cell. Each grid cell includes the following parameters: center $x$, center $y$, width, height, and confidence score for the bounding box. The output feature of YOLO can be used to calculate a vector of $S \times S \times (5B + C)$ numbers for each image, where $S$ is the grid size including the width and height of the final feature maps, $B$ is the number of anchor boxes, and $C$ is the number of classes. In this study, the values were as follows: $S = 13$, $B = 2$, and $C = 1$. We used an initial learning rate of 0.001, which was decayed by a factor of 10 each time the validation loss plateaued after an epoch. We selected the model with the lowest validation loss. The computation time of the model per image was 0.05 s to 0.5 s.

### Temporal validation dataset

To validate the clinical performance of our model to detect pneumothorax, a temporal validation dataset was

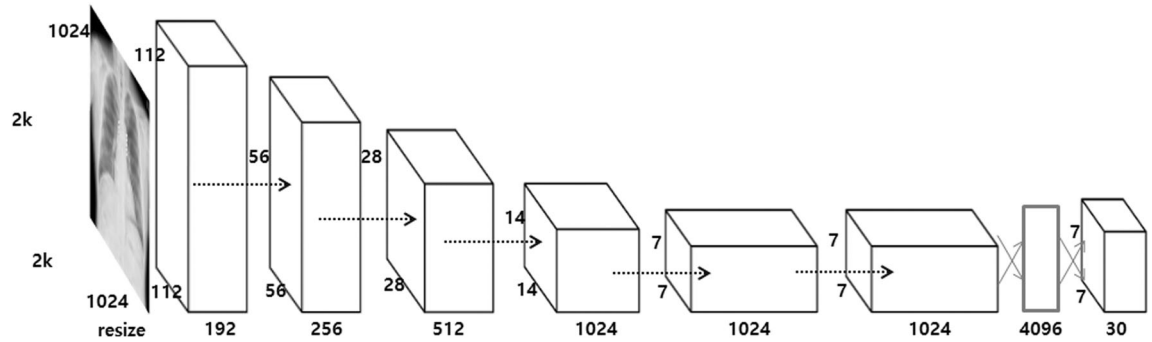


**Fig. 1** Architecture of a convolutional neural network. The proposed CNN architecture comprises 23 convolutional layers, each having a 3 × 3 kernel. To maintain original resolution throughout the network, we excluded a max pooling layer in the CNN structure and used the original matrix size of 1024 × 1024 for both input and output images

prepared using chest radiographs after PTNB. One radiologist (S.P. with 2 years of experience in chest CT) searched cases that were referred to the department of radiology in our hospital between January 2016 and December 2016. A total of 1462 PTNBs were found. Sixty-seven cases that were not for pulmonary lesions such as mediastinal, pleural, and chest wall lesions were excluded. Six cases without biopsy needle insertion were also excluded. In these cases, the lesion disappeared or was obscured by pleural effusion, or the patient had refused the procedure. Finally, 1389 PTNBs performed for 1333 pulmonary lesions in 1319 patients were included in our study (Fig. 2). Of the 1319 patients, 727 were men (mean age, 65.2 ± 10.5 years) and 592 were women (mean age, 61.2 ± 11.7 years). The mean lesion size was 30.0 ± 18.3 mm. The demographics of the patients and baseline characteristics of the pulmonary lesions are summarized in Table 1.

The temporal validation dataset included follow-up chest radiographs at two different time points after PTNB (3-h follow-up [1389 chest radiographs]; 1-day follow-up [1343 chest radiographs]). During the review of chest radiographs, those of cases wherein a chest tube was inserted were excluded to avoid pneumothorax determination based on the

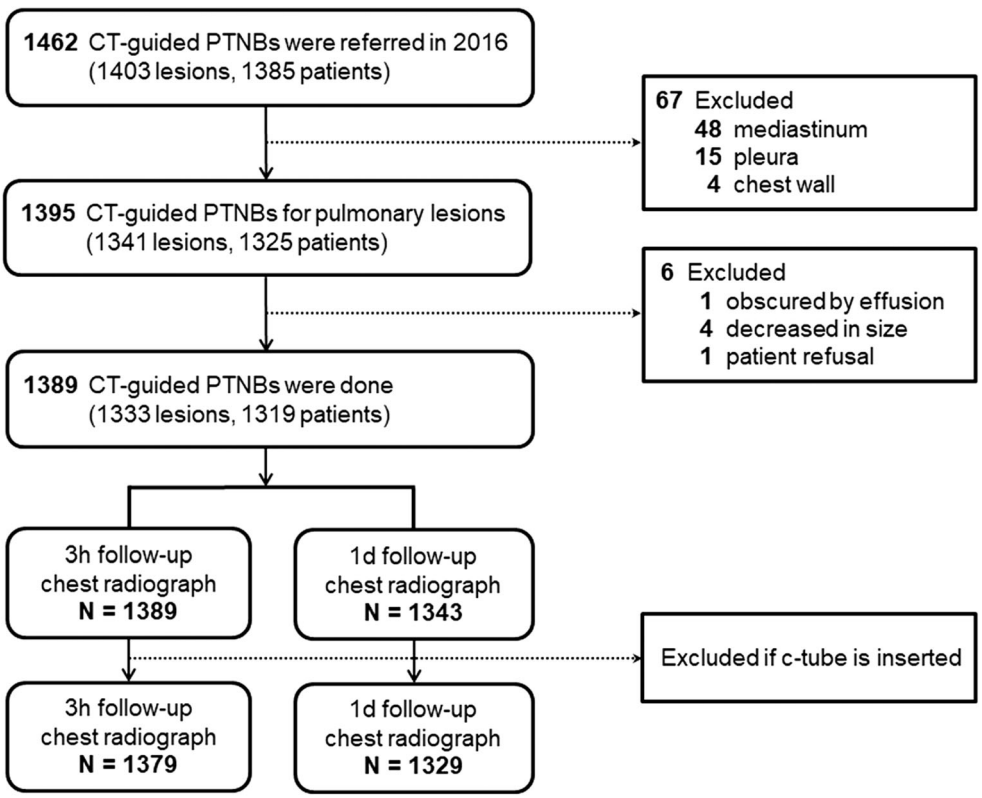


**Fig. 2** Flowchart illustrating the study inclusion process

**Table 1** Baseline characteristics of 1319 patients and 1333 pulmonary lesions with CT-guided percutaneous transthoracic biopsies

| Characteristic | |
|---|---|
| Age, years, mean ± SD | 63.4 ± 11.2 |
| Sex, *n* (%) | |
| Male | 727 (55.1) |
| Female | 592 (44.9) |
| Size, mm, mean ± SD | 30.0 ± 18.3 |
| Location, *n* (%) | |
| RUL | 343 (25.7) |
| RML | 86 (6.5) |
| RLL | 314 (23.6) |
| LUL | 323 (24.2) |
| LLL | 267 (20.0) |

Data are presented as mean ± standard deviation or *n* (%), unless indicated otherwise

*SD* standard deviation, *RUL* right upper lobe, *RML* right middle lobe, *RLL* right lower lobe, *LUL* left upper lobe, *LLL* left lower lobe

presence of a chest tube. Finally, 1379 3-h follow-up chest radiographs and 1329 1-day follow-up chest radiographs were selected for analysis.

### Biopsy procedure and follow-up

All PTNBs were performed by three fellows under supervision or by five chest faculties with more than 4 years of experience in chest intervention. CT-guided PTNB procedures were performed using a 64-MDCT (Somatom Definition AS; Siemens Healthcare). The CT parameters were 100 kVp, 25 mA reference, and 1.2 mm collimation with 1.5 mm axial slice thickness.

The standard coaxial technique was used with a 19-G coaxial introducer and a 20-G cutting needle (Pro-Mag 2.2; Manan Medical Products). Routinely, an immediate follow-up chest radiograph was obtained 3 h after the procedure. If no complication was identified on this exam, follow-up chest radiographs were obtained at intervals of 1 day. If pneumothorax was detected, the follow-up interval was shortened and a chest tube was inserted when clinically indicated. All chest radiographs were taken in an upright posteroanterior position.

### Reference standard

The reference standard for the presence of pneumothorax was determined by one radiologist (K.D. with 16 years of experience in thoracic radiology), reviewing serial chest radiographs and CT images obtained during the procedure. For equivocal determination of the presence of pneumothorax, another radiologist (S.M.L.) reviewed the chest radiographs. In such cases, pneumothorax was identified by consensus.

### Statistical analysis

The diagnostic performance of the CNN model for pneumothorax detection was compared to that of a reference standard using the jackknife free-response receiver operating characteristic (JAFROC) method. Sensitivity, specificity, and overall accuracy were calculated and compared between the 3-h and 1-day follow-up radiographs using chi-square tests.

All statistical analyses were performed using MedCalc statistical software (MedCalc Software, version 18.2.1). Data are presented as mean ± standard deviation. $P$ values $< 0.05$ were considered statistically significant.

## Results

### Incidence of pneumothorax after PTNB

Pneumothorax was detected at the 3-h follow-up in 247 cases (17.9%, 247/1379) and at the 1-day follow-up in 309 cases (23.3%, 309/1329). Six cases required immediate drainage catheter insertion after 3-h follow-up chest radiographs, and additional 17 cases required subsequent drainage catheter insertion after 1-day follow-up chest radiographs for the reason that pneumothorax persists or increases in amount. The 23 cases requiring chest tube insertion due to post-PTNB pneumothorax accounted for 6.6% of the 349 cases of pneumothorax observed on the 3-h or 1-day follow-up chest radiographs and 1.7% of the 1389 biopsies.

### Internal validation using the test dataset

To evaluate and validate our CNN model for the detection of pneumothorax, we used pneumothorax data of 253 patients and normal data of 250 patients. The sensitivity and specificity of pneumothorax detection were 89.7% (227/253) and 96.4% (241/250), respectively. The AUC was 0.984 (Fig. 3).

### Diagnostic yield using the temporal dataset

The diagnostic yields of the CNN model for the detection of pneumothorax are shown in Table 2. The CNN had 61.1% sensitivity (151/247), 93.0% specificity (1053/1132), 65.7% positive predictive value (151/230), 91.6% negative predictive value (1053/1149), and 0.898 AUC for 3-h follow-up chest radiographs and 63.4% sensitivity (196/309), 93.5% specificity (954/1020), 74.8% positive predictive value (196/262), 89.4% negative predictive value (954/1067), and 0.905 AUC for 1-day follow-up chest radiographs. There was no significant difference in the diagnostic performance between chest radiographs obtained at the 3-h and 1-day follow-up time points ($p = 0.578$ and 0.639 for sensitivity and specificity, respectively). Figure 3 presents two JAFROC curves

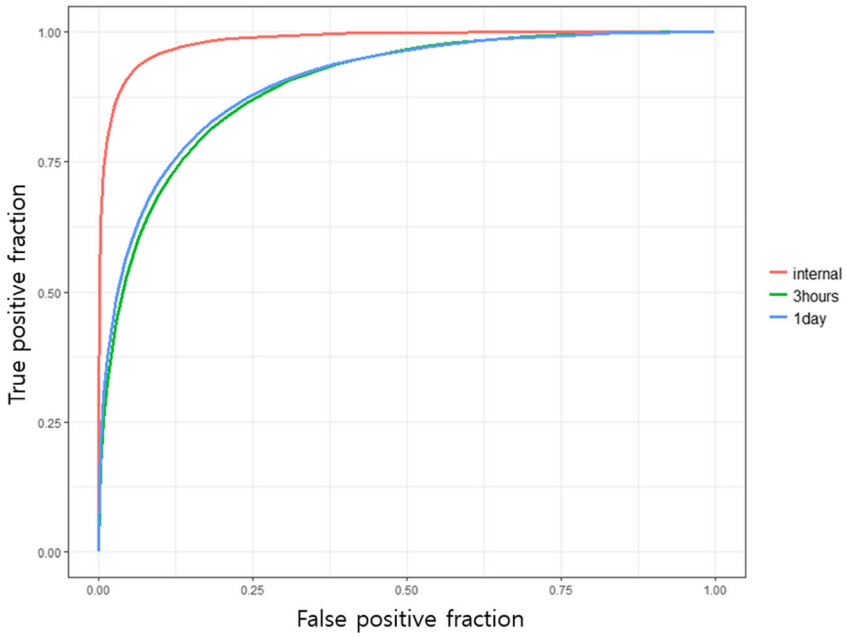


**Fig. 3** JAFROC analysis for the detection of pneumothorax. The JAFROC curves for internal validation (blue), 3-h follow-up chest radiographs (green), and 1-day follow-up chest radiographs (red) show the corresponding AUCs of 0.984, 0.898, and 0.905

illustrating algorithm performance as the predictive probability threshold at the 3-h and 1-day follow-up time points. The overall accuracy was 87.3% (1204/1379) for the 3-h follow-up and 86.5% (1150/1329) for the 1-day follow-up. There was no significant difference in accuracy ($p = 0.548$).

The CNN model detected all six cases requiring chest tube insertion on the same day based on the 3-h follow-up chest radiographs (Fig. 4), as well as all 17 cases eventually requiring chest tube insertion later based on the 1-day follow-up chest radiographs.

## Discussion

Our study is the first large study to evaluate the performance of a CNN model for detection of pneumothorax in a specific clinical scenario. Our CNN model detected pneumothorax with good performance on post-PTNB follow-up chest radiographs (AUC = 0.898 and 0.905 for 3-h and 1-day follow-up time points, respectively) and had especially high specificity and negative predictive value.

Previous studies using deep learning algorithms have reported high sensitivity (78–95.4%) and specificity (78–87%) for diagnostic models used for pneumothorax detection on chest radiographs [5, 7, 8]. Although the internal validation results of our model were comparable or slightly superior to the above models, the temporal validation results of our model showed lower sensitivity (61.1–63.4%) and slightly higher specificity (93.0–93.5%). Several possible explanations may account for this observation.

First, the severity of pneumothorax in patients with PTNB may be less than that in other populations. Given the need for very large datasets for deep learning model development, our study and those of others have collected chest images of patients with pneumothorax from multiple heterogeneous sources rather than those from samples with consecutive recruitment. This may lead to spectrum bias [10]. Specifically, severer or more easily detected cases of pneumothorax are more likely to be included in the datasets when compared to cases of pneumothorax of low severity on chest radiographs. In fact, our first CNN model detected fewer than 20% of the cases of pneumothorax on post-PTNB chest radiographs. We achieved the present sensitivity after the inclusion of pneumothorax cases occurring after PTNB performed in 2014 for model training.

Considering the differences between our internal and external validation results, other models should also be assessed externally in a specifically defined population. The results of

**Table 2** Performance of the deep learning–based model in pneumothorax detection

| | Sensitivity (%) | Specificity (%) | Accuracy (%) | AUC |
|---|---|---|---|---|
| Internal validation | 89.7 (227/253) | 96.4 (241/250) | 93.0 (468/503) | 0.984 |
| Pneumothorax after 3 h | 61.1 (151/247) | 93.0 (1053/1132) | 87.3 (1204/1379) | 0.898 |
| Pneumothorax after 1 day | 63.4 (196/309) | 93.5 (954/1020) | 86.5 (1150/1329) | 0.905 |

*AUC* area under the curve

such studies cannot be guaranteed when applying the diagnostic model to a population comprising difficult cases with pneumothorax of low severity.

In this context, external validation is crucial when assessing diagnostic performance while avoiding over-estimation. We thus selected one clinical scenario comprising post-PTNB follow-ups with clear inclusion criteria and a newly recruited study population as a validation dataset temporally separated from the training dataset. We believe that our results would allow us to predict real clinical performance.

Second, the prevalence of pneumothorax in our study was less than that in other validation datasets, with the exception of that in the study by Cicero et al [7]. Previous researchers have trained and tested their models in populations with high prevalence of pneumothorax. Although this may be easy-to-develop CNN models, it carries a risk of decreased performance in external validation with different disease prevalence rates [10]. In our study, the pneumothorax rates were 17.9% (247/1379) and 23.3% (309/1329) on 3-h and 1-day follow-up chest radiographs, respectively. These rates are within the range of previously reported pneumothorax rates (17.0–38.3%) [1, 3, 4].

Lastly, as the training dataset and the internal validation dataset were collected from two different hospitals, it is possible that our CNN model learned to identify subtle differences in radiographs of the hospitals. This type of training would affect the performance in test datasets from a single hospital, which would explain why it performs worse on our temporal validation set.

There were 96 and 113 false-negative cases and 79 and 66 false-positive cases at the 3-h and 1-day follow-up time points, respectively (Fig. 5). The main confounders in the false-negative cases were overlap with rib margins, concomitant effusion, and obscuring of some parts of the pleural lining due to parenchymal lesions such as masses, consolidation, and fibrosis. Localized pneumothorax at non-apex locations ($n = 4$), which was not observed in the training dataset, was also missed. In cases of pneumothorax of very low severity, the reduced size of images at the time of input may have contributed to missed detection because the pleural line can be very subtle even on the original images. Mimickers of pneumothorax in the false-positive cases were pleural thickening, sclerotic rib margins, medial borders of scapula, and skin folds. This suggests that the CNN model predicted the presence of pneumothorax in cases with transverse linear opacity similar to the pleural lining in the background of hypodense lungs.

Considering the false-positive results, there is room for improvement in the accuracy of the CNN model. Better specificity would be achieved if a large number of negative cases, including cases of pneumothorax mimickers, are provided to the model as negative controls and if the ability to compare the contralateral lung is incorporated into the training. Similarly, training through a large number of positive cases including varying severity of pneumothorax in various locations, not just the apex, may help improve sensitivity.

In cases of drainage of pneumothorax, physicians usually decide whether further procedures are necessary, considering the amount and duration of the pneumothorax, the patient's clinical condition, symptom, and underlying disease. Therefore, it may be difficult to define the clear-cut timing and specific indications for chest tube drainage. Nevertheless, based on the result that all cases requiring subsequent drainage tube insertion were detected, our CNN model has potential for use to detect pneumothorax cases requiring definite clinical alerts, such as that in patients with underlying diseases including emphysema or interstitial lung disease.

Although they performed their study using a different modality and in a different organ, Prevedello et al [11] have already demonstrated that deep learning–based automated identification of critical findings on non-contrast brain CT is feasible and could be used to notify radiologists of crucial

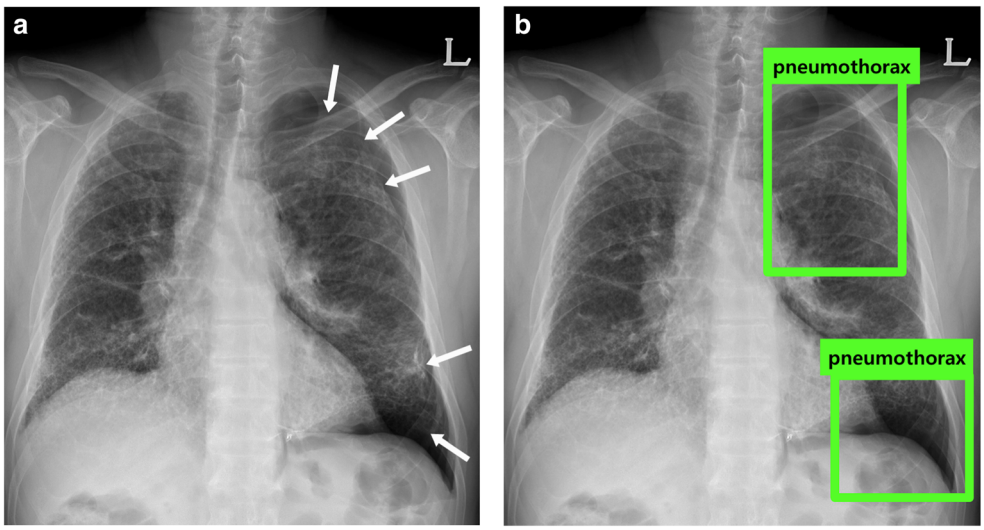


**Fig. 4** Rapid progression of pneumothorax after biopsy. A 60-year-old man with underlying usual interstitial pneumonia underwent PTNB for a 30-mm irregular nodule in the left lower lung field. After biopsy, the patient complained of aggravation of dyspnea. Post-PTNB chest radiograph after 3 h (**a**) revealed newly developed moderate amount of left pneumothorax. Chest tube insertion for drainage was performed. **b** Our deep learning–based model successfully detected pneumothorax in the patient

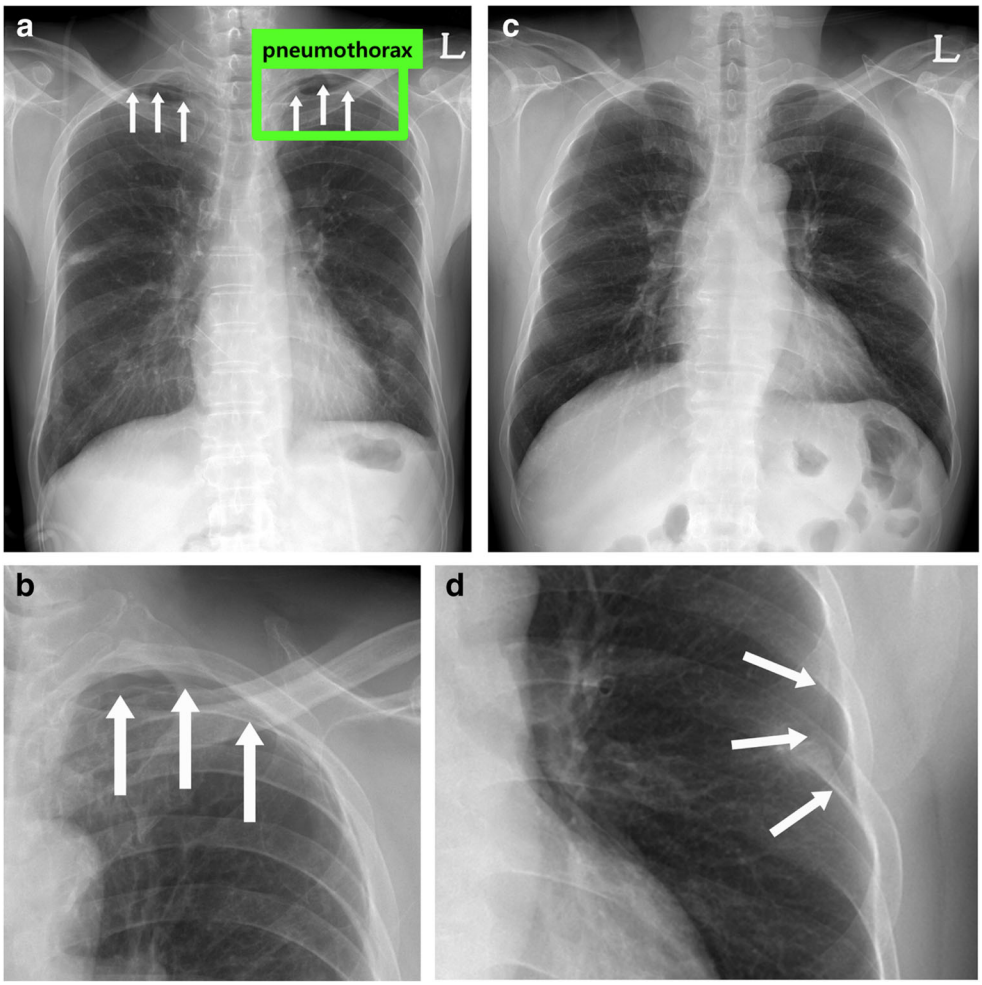


**Fig. 5** False-positive and false-negative cases of the deep learning–based network model. **a** A 63-year-old man with biopsy-proven organizing pneumonia in the right upper lobe. The CNN model classified the image as positive for pneumothorax in the apex of the left lung based on the 1-day follow-up chest radiograph after PTNB. In this case, the sclerotic change in the posterior arc of the left third rib was probably mistaken for a pleural line. Clinical information regarding the biopsy site and comparison of bilateral bone changes (arrows) may help observers determine that it was not a pleural line suggesting pneumothorax. **b** A 71-year-old man with a 17-mm squamous cell carcinoma in the left upper lobe. A pneumothorax of very low severity in the apex of the left lung (arrow) on the 1-day follow-up chest radiograph was missed by the CNN model. **c**, **d** A 55-year-old male with adenocarcinoma in the lingular segment of the left upper lobe. Localized pneumothorax was observed in the left middle lung zone (arrow) on the 1-day follow-up chest radiograph. This was missed by the CNN model

findings. In the above study, the final algorithm had 90% (45/50) sensitivity, 85% (68/80) specificity, and an AUC of 0.91 for the detection of hemorrhages, mass effects, and hydrocephalus. The same strategy can be used during post-PTNB follow-ups to increase the efficiency of clinical workflow. In addition, as suggested by the high negative predictive value, this model can be used as a screening tool to exclude cases without complications and to identify cases requiring additional confirmation by radiologists. Moreover, different levels of notifications can be possible if the detected extent of pneumothorax is accurate and quantifiable or classifiable.

Our study has several limitations. First, chest CT, which is the gold standard diagnostic test for pneumothorax, was not available for all post-PTNB cases. Instead, we used the two experienced radiologists' diagnosis as a reference standard, although this may be somewhat subjective. In practice, however, most cases of pneumothorax do not require additional confirmation by CT and are diagnosed based on radiography. Second, we collected the temporal validation dataset from the facility that provided the training dataset. Although the two datasets were temporally separated, the performance of the CNN model may be affected. Therefore, to verify our results, further studies including data from different facilities are warranted. Lastly, our dataset did not include multiple heterogeneous sources such as those from different machines utilizing different methods of image acquisition and post-processing. However, we obtained

datasets from two medical centers using different reconstruction methods. The limitations of the single-center study have thus been overcome in some extent. Further validation is warranted before our model can be used more generally.

In conclusion, our CNN model had good performance for detection of pneumothorax on chest radiographs after PTNB, especially for those requiring further procedures. It can be used as a screening tool prior to radiologist interpretation.

**Funding** The authors received funding for this study from the Industrial Strategic Technology Development program (10072064, Development of Novel Artificial Intelligence Technologies to Assist Imaging Diagnosis of Pulmonary, Hepatic, and Cardiac Diseases and Their Integration into Commercial Clinical PACS Platforms) funded by the Ministry of Trade Industry and Energy (MI, Korea).

## Compliance with ethical standards

**Guarantor** The scientific guarantor of this publication is Sang Min Lee.

**Conflict of interest** The authors declare that they have no competing interests.

**Statistics and biometry** No complex statistical methods were necessary for this paper.

**Informed consent** Written informed consent was waived by the institutional review board.

**Ethical approval** Institutional review board approval was obtained.

**Methodology**
- retrospective
- diagnostic or prognostic study
- performed at one institution

## References

1. Geraghty PR, Kee ST, McFarlane G, Razavi MK, Sze DY, Dake MD (2003) CT-guided transthoracic needle aspiration biopsy of pulmonary nodules: needle size and pneumothorax rate. Radiology 229(2):475–481
2. Hiraki T, Mimura H, Gobara H et al (2009) CT fluoroscopy-guided biopsy of 1,000 pulmonary lesions performed with 20-gauge coaxial cutting needles: diagnostic yield and risk factors for diagnostic failure. Chest 136(6):1612–1617
3. Lee SM, Park CM, Lee KH, Bahn YE, Kim JI, Goo JM (2014) C-arm cone-beam CT-guided percutaneous transthoracic needle biopsy of lung nodules: clinical experience in 1108 patients. Radiology 271(1):291–300
4. Yeow KM, Su IH, Pan KT et al (2004) Risk factors of pneumothorax and bleeding: multivariate analysis of 660 CT-guided coaxial cutting needle lung biopsies. Chest 126(3):748–754
5. Geva O, Zimmerman-Moreno G, Lieberman S, Konen E, Greenspan H (2015) Pneumothorax detection in chest radiographs using local and global texture signatures. SPIE Proceedings, Vol. 10575
6. Chan YH, Zeng YZ, Wu HC, Wu MC, Sun HM (2018) Effective pneumothorax detection for chest X-ray images using local binary pattern and support vector machine. J Healthc Eng 2018:11
7. Cicero M, Bilbily A, Colak E et al (2017) Training and validating a deep convolutional neural network for computer-aided detection and classification of abnormalities on frontal chest radiographs. Invest Radiol 52(5):281–287
8. Blumenfeld A, Konen E, Greenspan H (2018) Pneumothorax detection in chest radiographs using convolutional neural networks. SPIE Proceedings, Vol. 10575
9. Redmon J, Farhadi A (2016) YOLO9000: better, faster, stronger. IEEE Conference on Computer Vision and Pattern Recognition (CVPR), 6517–6525
10. Park SH, Han K (2018) Methodologic guide for evaluating clinical performance and effect of artificial intelligence technology for medical diagnosis and prediction. Radiology 286(3):800–809
11. Prevedello LM, Erdal BS, Ryu JL et al (2017) Automated critical test findings identification and online notification system using artificial intelligence in imaging. Radiology 285(3):923–931